Ca transients in cardiac myocytes measured with a low affinity fluorescent indicator, furaptra

M. Konishi and J. R. Berlin
Bockus Research Institute, Graduate Hospital, Philadelphia, Pennsylvania 19146 USA

ABSTRACT Intracellular calcium ion ($[Ca^{2+}]_i$) transients were measured in single rat ventricular myocytes with the fluorescent indicator furaptra. Cells were voltage clamped with a single patch electrode containing the K^+ salt of furaptra and fluorescence at 500 nm was measured during illumination with 350 and 370 nm light. Depolarizing voltage-clamp pulses elicited $[Ca^{2+}]$-dependent fluorescent transients in 30 of 33 cells tested. The peak change in $[Ca^{2+}]_i$ elicited by 50-ms depolarizations from −70 to +10 mV was 1.52 ± 0.25 μM (mean ± SEM, n = 7). The size of the $[Ca^{2+}]_i$ transient increased in response to 10 μM isoproterenol, prolongation of the depolarization, and increasing pipette $[Na^+]$. Because furaptra is sensitive to Ca^{2+} and Mg^{2+}, changes in $[Mg^{2+}]_i$ during the $[Ca^{2+}]_i$ transient could not be measured. Instead, a single-compartment model was developed to simulate changes in $[Mg^{2+}]$ during $[Ca^{2+}]$ transients. The simulations predicted that a 2 μM $[Ca^{2+}]$ transient was accompanied by a slow increase in $[Mg^{2+}]$ (14–29 μM), which became larger as basal $[Mg^{2+}]$ increased (0.5–2.0 mM). The $[Mg^{2+}]$ transient reached a peak ~1 s after the peak of the $[Ca^{2+}]$ transient with the slow changes in $[Mg^{2+}]$ dominated by competition at the Ca^{2+}/Mg^{2+} sites of Troponin. These changes in $[Mg^{2+}]$, however, were so small and slow that they were unlikely to affect the furaptra fluorescence signal at the peak of the $[Ca^{2+}]_i$ transient. The $[Ca^{2+}]_i$ transient reported by furaptra appears to be larger than that reported by other Ca^{2+} indicators; however, we conclude this larger transient is at least as accurate as $[Ca^{2+}]_i$ transients reported by the other indicators.

INTRODUCTION

The central role of intracellular calcium ion concentration ($[Ca^{2+}]_i$) in controlling heart contractile function has motivated the development of a variety of experimental methodologies to measure $[Ca^{2+}]_i$ in cardiac myocytes. The most versatile of these methods uses Ca^{2+}-sensitive optical indicators, such as aequorin (1), which allow rapid changes in $[Ca^{2+}]_i$ to be observed. The introduction of the ratiometric Ca^{2+} indicators, fura-2 and indo-1 (2), has led to a dramatic improvement in the ability to measure changes in $[Ca^{2+}]_i$ because, unlike aequorin, these fluorescent indicators form a 1:1 complex with Ca^{2+} and have Ca^{2+}-binding affinities close to physiological $[Ca^{2+}]_i$. More recently several nonratiometric Ca^{2+} indicators have also been introduced.

Concerns have been raised about quantitation of $[Ca^{2+}]_i$ in heart muscle with some of these new Ca^{2+} indicators because their Ca^{2+}-binding and optical properties appear to be different in the intracellular environment than in *in vitro* conditions. A sizable fraction of fura-2 and indo-1 is bound in the intracellular environment (3–5), and this binding appears to affect the Ca^{2+}-indicator properties of these compounds (3, 5). Another concern is that the reaction kinetics of fura-2 are too slow to accurately track rapid changes in $[Ca^{2+}]_i$ that occur during the stimulated $[Ca^{2+}]_i$ transient, as has been reported in skeletal muscle fibers (6, 7). Finally, in the presence of spatial gradients of $[Ca^{2+}]_i$ (8, 9), it is not clear that fura-2 gives an accurate measure of spatial mean $[Ca^{2+}]_i$ because of possible saturation of the indicator in the regions of high $[Ca^{2+}]_i$ (10).

The potential complexities in relating changes in fura-2 fluorescence to $[Ca^{2+}]$ point out the advantages in having a variety of Ca^{2+} indicators with different Ca^{2+}-binding properties to check the accuracy of Ca^{2+} measurements made in cardiac cells with more commonly used indicators such as fura-2 and indo-1. Recently, Konishi et al. (11) demonstrated that furaptra, a fluorescent indicator originally designed to measure Mg^{2+} (12), can be used to measure the rapid changes in $[Ca^{2+}]_i$ that occur in skeletal muscle fibers. Preliminary data also suggested that Ca^{2+}-dependent changes in furaptra fluorescence could be measured in cardiac myocytes; however, these changes were unreliable due to movement artifacts that obscured Ca^{2+}-dependent changes in fluorescence (13).

In this report, we demonstrate that furaptra can reliably be used to measure the amplitude of the $[Ca^{2+}]_i$ transient in cardiac myocytes. We present a method to calibrate Ca^{2+}-dependent changes in furaptra fluorescence and estimate the degree to which Mg^{2+}-dependent changes in fluorescence complicate measurement of $[Ca^{2+}]_i$.

Some of the data have been previously published in abstract form (14, 15).

MATERIALS AND METHODS

General

The experimental techniques used in this study are modifications of previously published methods (16). Single ventricular myocytes were enzymatically isolated from rat hearts by a modification of the method of Mitra and Morad (17). After enzymatic digestion and dispersion, cells were stored in a 0.2 mM $CaCl_2$-containing Tyrode's solution at

M. Konishi's present address is Department of Physiology, The Jikei University School of Medicine, 3-25-8 Nishi-shinbashi, Minato-ku, Tokyo 105, Japan.

Address correspondence to J. R. Berlin, Bockus Research Institute, Graduate Hospital, 415 S. 19th St., Philadelphia, PA 19146, USA.

room temperature or at 6°C until used. Cells were placed in an experimental chamber (18) on the stage of an inverted microscope (Diaphot, Nikon Inc. Instrument Division, Garden City, NY) and superfused with a 2 mM $CaCl_2$ Tyrode's solution. Cells were voltage clamped via a single electrode technique (19) with patch pipettes of 1–2 MΩ resistance filled with a salt solution containing 0.3–1.0 mM furaptra or 50 μM fura-2 (both as the K^+ salt). After formation of a GΩ seal, zero current and background fluorescence were measured. The membrane patch under the pipette was then ruptured to establish a whole cell voltage clamp and allow indicator diffusion into the myocyte. Fluorescence measurements were carried out under conditions where dye loading was near steady-state levels.

Equipment for fluorescence measurement

Light from a xenon arc (PTI Inc., South Brunswick, NJ) was collected and partially collimated before passing through narrow-band interference filters (10 nm FWHM). The excitation wavelength was selected by moving two filters into the light path between consecutive depolarizations under the control of a stepper motor filter changer. The filtered light was then focused onto one end of a liquid light guide. The other end of the light guide was placed in the epifluorescence port of the microscope so that the image of the light guide formed by a divergent lens was at the back image plane of a high N.A. oil immersion objective, which focused the ultraviolet light onto the cell. Incident light was limited to the area of the cell with an adjustable field stop. An electronic shutter (Vincent Electronics, Rochester, NY) also limited the exposure of the cell to light for 1.0–1.5 s periods around each depolarization. The intensity of the excitation light was attenuated with neutral density filters until the half-time for bleaching of the indicator was ~90 s. Light from the Kohler illuminator of the microscope was used throughout the experiments to view the cell with a CCD camera (NEC Corp., Mountain View, CA) but was limited to wavelengths longer than 750 nm with a longpass interference filter.

Fluorescent light at 500 nm (40 nm FWHM) was measured with a photomultiplier tube (Thorn EMI, Rockaway, NJ) after separation of light with wavelengths longer than 700 nm by dichroic mirrors. A field stop limited the view of the photomultiplier to the area of the myocyte.

Membrane potential, current, and fluorescence were recorded on videotape (Instrutech VR-100, Elmont, NY). For analysis, recorded data was filtered at 500 Hz with an eight-pole Bessel filter and digitized at 1 kHz (DT2801A, Data Translation, Inc, Marlboro, MA) using commercially available software (A2D+; Medical Systems, Greenvale, NY). Fluorescence data presented in the figures are the signal average of consecutive traces from six to eight depolarizations at each illumination wavelength.

Calibration

In vitro calibrations of furaptra were carried out on the experimental apparatus with a glass capillary ~ 100 μm in diameter. The calibration solution contained 140 mM KCl, 1 μM furaptra (K^+ salt), and 10 mM PIPES (piperazine-*N*,*N*'-bis[2-ethanesulfonic acid]), pH 7.2. For calibration of calcium-dependent changes in fluorescence, 5 mM HEDTA (*N*-hydroxyethylethylenediaminetriacetic acid) and various amounts of $CaCl_2$ were added to set free Ca^{2+} concentrations. Magnesium-dependent fluorescence changes were determined in the presence of 0.2 mM K_2EGTA [ethylene glycol-bis(β-aminoethyl ether)*N*,*N*,*N*',*N*'-tetraacetic acid] to remove contaminant Ca^{2+}. Free magnesium concentration was set by dilution of a 1 M $MgCl_2$ stock solution without additional buffers. Free ion concentrations were calculated with a computer program, MaxChelator, version 4.61 (written by Chris Patton, Hopkins Marine Station, Pacific Grove, CA), that used the equations from Fabiato and Fabiato (20) and dissociation constants determined by Harrison and Bers (21) and Martell and Smith (22).

Solutions and materials

Myocytes were superfused with a Tyrode's solution containing (mM) 140 NaCl, 4 KCl, 1 $MgCl_2$, 2 $CaCl_2$, 10 glucose and 10 HEPES (*N*-[2-hydroxyethyl]piperazine-*N*'-[2-ethanesulfonic acid]), pH 7.4. All experiments were performed at room temperature. The internal electrode solution contained (mM): 70 cesium glutamate, 50 KCl, 15 CsCl, 1 $MgCl_2$, 2.5 ATP (K^+ salt), 0.01–0.07 EGTA, and 25 PIPES, pH 7.2.

All chemicals were reagent grade. Isoproterenol bitartrate was purchased from Sigma Chemical Co. (St. Louis, MO). The tetrapotassium salt of furaptra (Mag-fura-2, Lot 9A) and pentapotassium salt of fura-2 were purchased from Molecular Probes Inc. (Eugene, OR).

RESULTS

Furaptra has been previously reported to have fluorescent properties very similar to fura-2, with a significant blue shift in the excitation spectrum on metal binding, and an isosbestic point of 347 nm (12). Fig. 1 *A* shows furaptra fluorescence at different [Ca^{2+}] observed during an *in vitro* calibration on the experimental apparatus. Excitation with 340 or 350 nm light showed small Ca^{2+}-dependent changes in fluorescence in opposite directions, consistent with the isosbestic point being between these two excitation wavelengths. Konishi et al. (11) showed that the isosbestic point for furaptra is similar for Mg^{2+}- and Ca^{2+}-dependent changes in fluorescence. Fluorescence records in the remainder of the paper are presented under the assumption that records during 350 nm illumination represent fluorescence at the isosbestic point. Excitation at 370 nm showed a large Ca^{2+}-dependent decrease in fluorescence. At saturating Ca^{2+}, fluorescence intensity was ~10% of that observed in zero Ca^{2+} solution, consistent with Konishi et al. (11), who showed that the extinction coefficient (at 420 nm) is greatly decreased upon complexation with Ca^{2+}. To determine the K_D for Ca^{2+}, a 1:1 binding curve was fitted by a nonlinear least-squares routine to the fluorescence data measured with 370 nm excitation light. From the curve (Fig. 1 *A*), K_D for Ca^{2+} was calculated to be 58 μM. In a total of three calibrations, average K_D(Ca) equaled 47 ± 6 μM (mean ± SEM), very similar to the published values (Raju et al. (12), 53 μM at 37°C; Konishi et al. (11), 44 μM at 16°C).

Fig. 1 *B* shows the Mg^{2+}-dependent changes in furaptra fluorescence during excitation with 370 nm light. The Ca^{2+} concentration was maintained at low levels with 0.2 mM EGTA and Mg^{2+} concentration was varied by adding $MgCl_2$ to a HEPES-buffered solution at pH 7.2. A K_D of 3.6 mM (23°C) was calculated by the same method described in part *A* of the figure (*solid curve*). This fitted value of K_D(Mg) is intermediate between 1.5 mM at 37°C, reported by Raju et al. (12), and 5.3 mM at 16°C, reported by Konishi et al. (11).

Furaptra fluorescence transients

Given the low affinity of furaptra for Ca^{2+}, we expected that Ca^{2+}-dependent changes in fluorescence would be

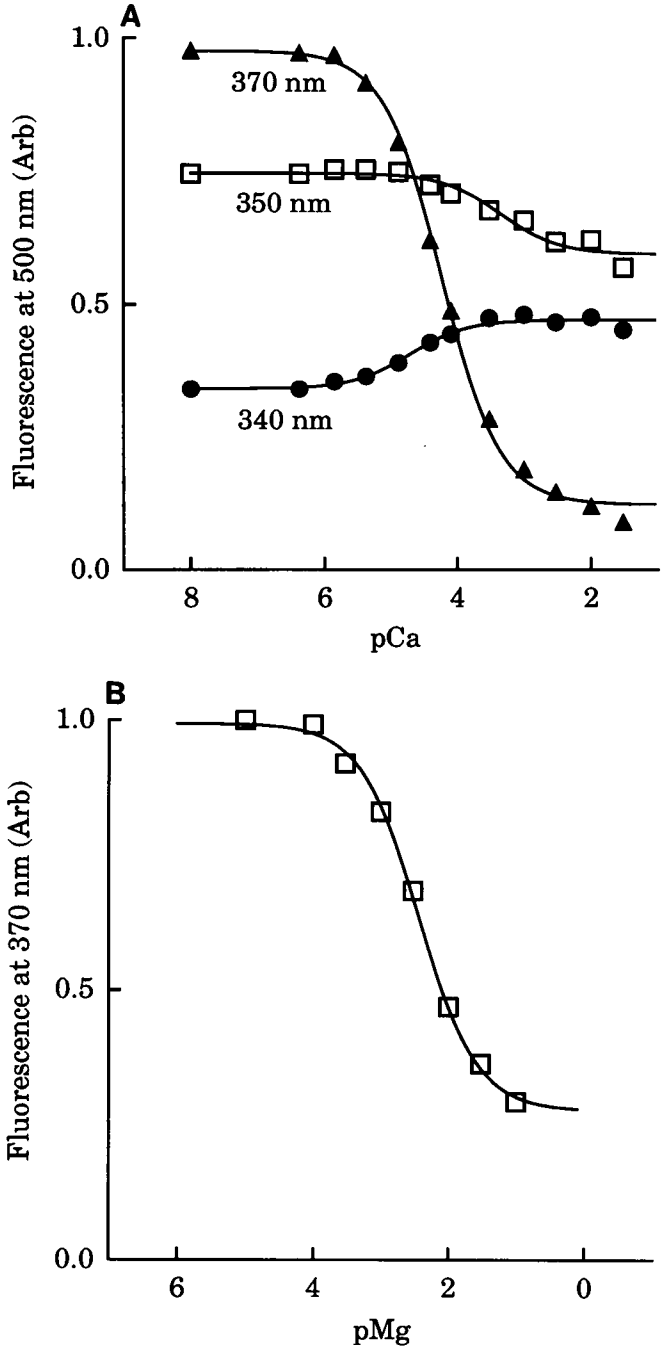

FIGURE 1 Ion dependence of furaptra fluorescence. Calibrations were carried out in the experimental chamber using 100 μm inside diameter glass capillaries that contained (mM) 140 KCl, 0.001 furaptra (K^+ salt), and 10 PIPES, pH 7.2 at room temperature. (*A*) Ca^{2+} dependence of fluorescence. 5 mM HEDTA and various amounts of $CaCl_2$ were used to set the $[Ca^{2+}]$. The capillary was illuminated with 340 nm (*circles*), 350 nm (*squares*), or 370 nm light (*triangles*) and fluorescence measured at 500 nm. The solid lines through the data were determined by nonlinear least-squares fit assuming 1-to-1 binding. (*B*) Mg^{2+} dependence of fluorescence measured with 370 nm illumination. Various amounts of $MgCl_2$ were added with 0.2 K_2EGTA to the basic solution to yield the desired $[Mg^{2+}]$. The solid line was least-squares-fit as in *A*.

quite small, 0.5–2.0%, because the peak change in $[Ca^{2+}]_i$ during a stimulated transient has been reported to be 250–1,000 nM (16, 23). We also anticipated that movement artifacts would pose a serious problem, as has been reported by Cleeman and Morad (13). For these reasons, attempts were made to improve the signal-to-noise ratio of the fluorescence signal by 1) use of high indicator concentrations (0.3 or 1.0 mM) in the patch electrode solution, 2) collection of the fluorescence signal from almost the entire area of the cell, and 3) signal averaging six to eight fluorescence records. Given these conditions, fluorescent transients could reliably be elicited by voltage-clamp depolarizations with almost every cell [30 of 33 cells examined in this study and Berlin and Konishi (15)]. The three cells that did not show any $[Ca^{2+}]_i$-dependent fluorescence transients also showed little or no contraction in response to voltage-clamp depolarizations. In voltage-clamped myocytes loaded with fura-2, we observe a similar percentage of cells in which $[Ca^{2+}]_i$ transients cannot be elicited. Thus, we find that furaptra can be used reliably to measure stimulated $[Ca^{2+}]_i$ transients.

Figs. 2 and 3 illustrate furaptra fluorescence transients and their conversion to changes in $[Ca^{2+}]_i$. In Fig. 2 *A*, the cell was depolarized from −70 to +10 mV for 500 ms (*top panel*) at 0.2 Hz. When fluorescence was measured during excitation with 350 nm light (*second panel*), the voltage clamp pulse produced a fluorescence transient that increased slowly, remained elevated for the duration of the depolarization, and returned to resting levels after repolarization. From Fig. 1, it is clear that this change in fluorescence is in the opposite direction of those anticipated from an increase in $[Ca^{2+}]_i$. It is also unlikely that this change in fluorescence reflects a change in intracellular $[Mg^{2+}]$ (see Fig. 6); however, the change does roughly parallel the time course expected for cell contraction. The interpretation that the signal during 350 nm illumination reflects a movement artifact is supported by the finding that depolarizations of 50 ms duration produce a fluorescent transient of shorter duration. This change is consistent with the absence of a tonic component of cell contraction with a 50-ms depolarization which could be present with a 500-ms depolarization. Thus, the changes in fluorescence measured with 350 nm illumination, a wavelength close to the isosbestic point, most likely reflect cell movement.

The third panel of Fig. 2 *A* shows the fluorescence transient recorded during illumination with 370 nm light. A rapid decrease in furaptra fluorescence is followed by a slower increase in fluorescence intensity that lasted the duration of the depolarization. The rapid decrease in fluorescence intensity is consistent with an increase in $[Ca^{2+}]_i$; however, as above, the prolonged increase in fluorescence is in the opposite direction of expected for either an increase in Ca^{2+} or Mg^{2+}.

Artifacts due to cell movement can, in principle, be removed by taking the ratio of fluorescence intensities at

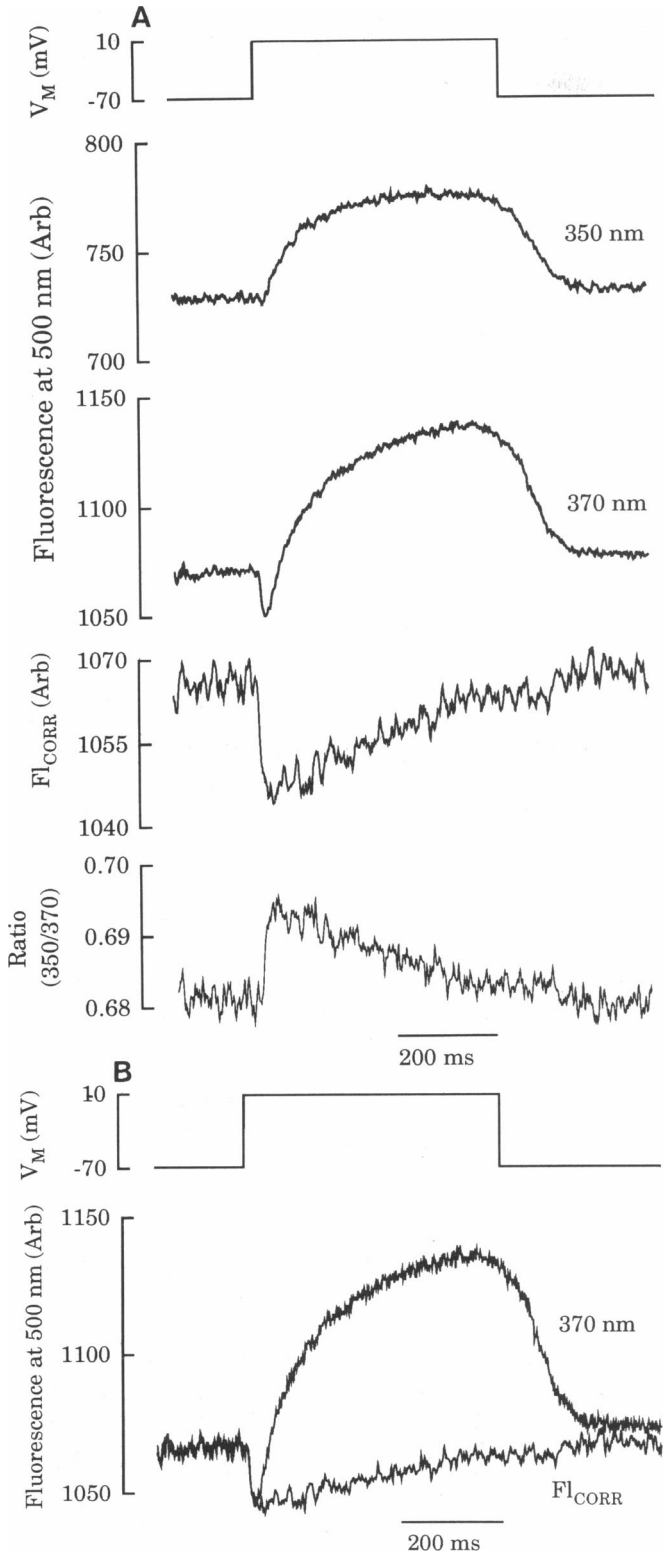

FIGURE 2 Calibration of fluorescence signals. (*A*) Removal of movement artifact from fluorescence signals. *The top panel* shows the voltage clamp pulse which was delivered every 5 s. *The second and third panels* show the 500-nm fluorescence records (average of six depolarizations each) acquired during illumination at 350 and 370 nm, respectively, and displayed in arbitrary intensity units. *The fourth panel* shows the corrected fluorescence signal calculated as described in the text using Eq. 1. *The bottom panel* shows the ratio of fluorescence intensities measured during 350 and 370 nm illumination. (*B*) Comparison of the corrected and uncorrected fluorescence signal. *The top panel* shows the voltage-clamp depolarization. *The bottom panel* shows superimposed fluorescence records expressed in arbitrary intensity units. No scaling or offsets have been added to either record.

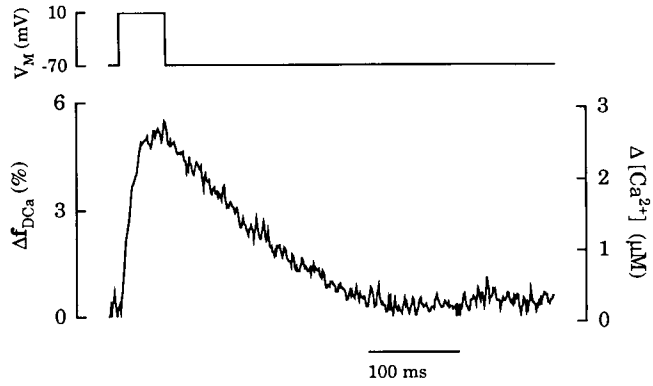

FIGURE 3 Calibration of furaptra fluorescence. *The top panel* shows the voltage-clamp depolarization. *The bottom panel* shows the corrected fluorescence transient resulting from signal-averaging fluorescence records from eight depolarizations with 350 and 370 nm illumination. The conversion to $\Delta[Ca^{2+}]_i$, as determined by Eq. 4, is shown on the righthand scale.

two illumination wavelengths (2). The fluorescence ratio signal of furaptra (*bottom panel* of Fig. 2 *A*) rises rapidly after membrane depolarization and reaches a peak within 30–35 ms. The signal then decreases back toward resting levels. The waveform of the ratio signal is consistent with anticipated changes in $[Ca^{2+}]_i$ during a transient. Conversion of the fluorescence ratio into $[Ca^{2+}]_i$, however, is complicated because the ratio is dependent on the degree of Ca^{2+} and Mg^{2+} binding to the indicator and the amount of Mg^{2+} bound to furaptra is likely to be much larger than the amount of bound Ca^{2+}. To overcome this problem, we have adopted an alternate method of calibration to correct for movement artifacts in the fluorescent signal measured during illumination with 370 nm light.

The alternative calibration method is summarized in Eqs. 1–4 below. To correct the 370 nm fluorescence signal for movement artifacts, it is assumed that changes in fluorescence at the isosbestic point (350 nm illumination) appear in an identical proportion in fluorescence signals measured with other illumination wavelengths.

$$Fl_{corr}(t) = Fl_{370}(t) \cdot M(t) \qquad M(t) = \frac{Fl_{350}(\text{rest})}{Fl_{350}(t)} \qquad (1)$$

$$Fl_{corr}(t) = \epsilon_f \cdot [D]_t + \epsilon_b \cdot [DCa]_t = \epsilon_f \cdot [D]_t \qquad (2)$$

$$\Delta f_D(t) = \frac{Fl_{corr}(t) - Fl_i}{Fl_{corr}(\text{rest}) - Fl_i} \qquad Fl_i = Fl_{corr}(\text{rest}) \cdot \frac{\epsilon_b}{\epsilon_f} \qquad (3)$$

Movement-corrected fluorescence (Fl_{corr}) is calculated by multiplying the fluorescence signal during 370 nm illumination [$Fl_{370}(t)$] by $M(t)$, the ratio of fluorescence recorded before the depolarization [Fl_{350}(rest)] and at time, t [$Fl_{350}(t)$], during 350 nm illumination (Eq. 1). Because changes in fluorescence during 350 nm illumina-

tion reflect cell movement, changes in $M(t)$ are inversely proportional to the size of the movement artifact. Fl_{corr}, shown in the fourth panel of Fig. 2 *A*, should reflect ion-dependent changes in fluorescence free of movement artifacts. Fl_{corr} is also the sum of the fluorescence signals from the Ca^{2+}-free (D) and Ca^{2+}-bound (DCa) forms of furaptra. However, *a*) the ratio of the fluorescence coefficients for the bound and free form of furaptra (ϵ_b/ϵ_f) determined during *in vitro* calibrations is small and *b*) [DCa]/[D] is very small, so that changes in the fluorescence signal arise almost exclusively from the changes in Ca^{2+}-free indicator concentration (Eq. 2). Therefore, a fractional change in fluorescence will correspond directly to a change in the fraction of Ca^{2+}-free indicator.

Eq. 3 relates changes in fluorescence to changes in the fraction of Ca^{2+}-free furaptra [$\Delta f_D(t)$]. The Ca^{2+}-sensitive component of the fluorescence signal [$Fl_{corr}(t) - Fl_i$] at time t is divided by the Ca^{2+}-sensitive component recorded before the voltage-clamp depolarization [$Fl_{corr}(\text{rest}) - Fl_i$], where the value of Fl_i is the expected fluorescence signal in saturating $[Ca^{2+}]_i$, i.e., the Ca^{2+}-insensitive fluorescence. Fl_i is calculated as the fluorescence before the depolarization [$Fl_{corr}(\text{rest})$] times the ratio of the fluorescence coefficients for the Ca^{2+}-bound and Ca^{2+}-free forms of furaptra.

Two underlying assumptions are implicit in the calculation of $\Delta f_D(t)$. First, $Fl_{corr}(\text{rest})$ is assumed to be the level of fluorescence with no Ca^{2+} binding. If resting $[Ca^{2+}]_i$ is 100 nM, then the Ca^{2+}-bound fraction of the indicator is only 0.5%, so that this assumption leads to only very small errors in calibration. Second, $[Mg^{2+}]_i$ must not significantly change during the $[Ca^{2+}]_i$ transient. This latter assumption is examined in Fig. 6.

Because $\Delta f_D(t)$ arises from Ca^{2+}-free furaptra, $1 - \Delta f_D(t)$ equals the change in the fraction of furaptra bound to Ca^{2+} [$\Delta f_{DCa}(t)$], which is directly proportional to the change in $[Ca^{2+}]_i$ ($\Delta[Ca^{2+}]_i$), as shown in Eq. 4:

$$\Delta[Ca^{2+}]_i = K_D \cdot [1 - \Delta f_D(t)] = K_D \cdot \Delta f_{DCa}(t). \quad (4)$$

This equation is essentially the same as Eq. 4 in Konishi et al. (11) but simplified because the fractional binding of furaptra with Ca^{2+} in the present experiments is small (usually $\leq 5\%$). K_D was determined *in vitro* as in Fig. 1 and adjusted for competition with Mg^{2+}. Intracellular Mg^{2+} concentration ($[Mg^{2+}]_i$) was not studied systematically during these experiments and was assumed to be 0.5 mM. This value is similar to that reported in several recent studies using furaptra (24), ion-selective electrodes (25), and ^{19}F-NMR (24). The adjusted K_D for Ca^{2+} is 54 μM.

The movement artifact in the fluorescence recorded during illumination with 370 nm light can often be as large or larger than the Ca^{2+}-dependent change in fluorescence (cf. *third panel* of Fig. 2 *A*). Ratiometric methods (including calculation of Fl_{corr}) are designed to remove the contribution of cell movement (or any change in effective pathlength) from the calibration process. Nonetheless, large movement artifacts may be difficult to completely remove, particularly with the experimental procedure used here, where the illumination wavelength is alternated with consecutive depolarizations. For this reason, we have more closely examined the potential for movement artifact to contribute to Fl_{corr} used in the calibration. Fig. 2 *B* shows the raw fluorescence signal recorded during 370 nm illumination superimposed on the Fl_{corr} signal. The initial change in fluorescence coincides closely for both signals. Correcting for the movement artifact delays the peak change in fluorescence of Fl_{corr} from 18 to 32 ms after the beginning of the depolarization and increases the amplitude from a 1.8 to a 2.0%. Thus, most of the rapid rising phase of the fluorescence transient occurs before onset of the movement artifact. Because the peak Ca^{2+}-dependent change in fluorescence occurs at a time when cell movement is only very slight, movement artifact correction alters the estimation of peak changes in $[Ca^{2+}]_i$ by 10%. On the other hand, the falling phase of the $[Ca^{2+}]_i$ transient and the tonic elevation of $[Ca^{2+}]_i$ occur during cell contraction. Thus, in later phases of the $[Ca^{2+}]_i$ transient recorded with furaptra, we have no independent verification that movement artifacts do not significantly alter the Fl_{corr} signal.

The above calibration method is used in Fig. 3 to convert Fl_{corr} to $\Delta[Ca^{2+}]_i$. The cell was depolarized from -70 to $+10$ mV for 50 ms every 5 s and the signal-averaged fluorescence transient is shown as Δf_{DCa}. The peak change in fluorescence is 5.2%, which converts into a peak $\Delta[Ca^{2+}]_i$ of 2.8 μM. Although this was one of the larger $[Ca^{2+}]_i$ transients observed, on average, the peak $\Delta[Ca^{2+}]_i$ was 1.52 ± 0.25 μM (mean $\pm$ SEM, $n = 7$), and the average time to peak change in $[Ca^{2+}]_i$ was 36 ± 3 ms.

To determine if the furaptra fluorescence transient (Δf_{DCa}) was consistent with the $[Ca^{2+}]_i$ transient expected for cardiac myocytes, we tested the effect of various experimental interventions on the size of the fluorescence transient. Fig. 4 *A* shows an experiment that examined the effect of isoproterenol, a β-adrenergic agonist expected to increase the size of the $[Ca^{2+}]_i$ transient in cardiac muscle (1). Before drug addition, the peak change in fluorescence in response to 50-ms depolarizations to +10 mV every 5 s was 1.6%, or a 0.86-μM increase in $[Ca^{2+}]_i$. After the addition of 10 μM isoproterenol to the superfusion solution, the fluorescence transient showed a peak change of 4.6% or a 2.48-μM increase in $[Ca^{2+}]_i$. Thus, in this cell, isoproterenol produced a 160% increase in the size of the $[Ca^{2+}]_i$ transient compared with control. In six cells, 10 μM isoproterenol led to an 84 ± 28% increase in the size of the fluorescence transient.

A second experimental maneuver was to increase the duration of the depolarizing voltage clamp pulse from 50

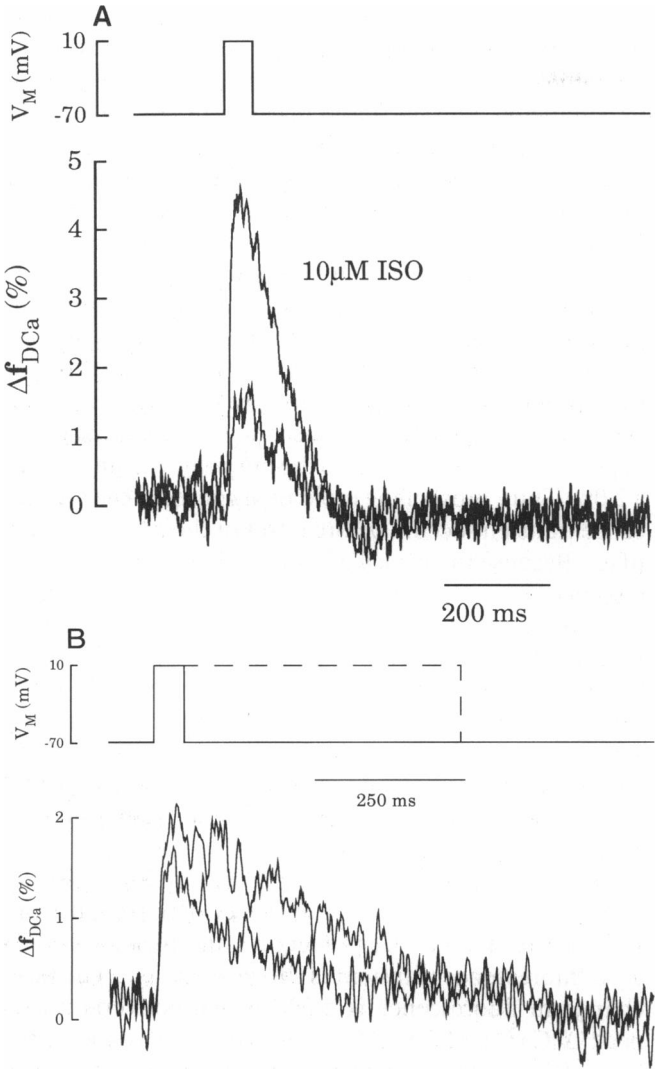

FIGURE 4 Effect of various interventions on the size of the furaptra fluorescence transient. (*A*) Isoproterenol. *The top panel* shows the voltage-clamp pulse used in this experiment. *The bottom panel* shows two superimposed corrected fluorescence transients recorded during superfusion with 0 and 10 μM isoproterenol. (*B*) Depolarization duration. Superimposed corrected fluorescence transients for 50- and 500-ms-long depolarizations from −70 to +10 mV delivered every 5 s. The transient resulting from the 500-ms-long voltage-clamp pulse has a higher peak change and a slower rate of recovery of fluorescence toward resting levels.

to 500 ms. The result of such an experiment is shown in Fig. 4 *B*, where fluorescence transients elicited by the two different depolarizations have been superimposed. The fluorescence transient arising from the 500-ms depolarization shows a larger peak amplitude. Increasing clamp pulse duration has been previously reported to increase the size of the $[Ca^{2+}]_i$ transient in myocytes loaded with fura-2 (13, 26) and indo-1 (27).

The third maneuver was to increase the NaCl concentration in the patch pipette solution from 0 to 8 mM. Maneuvers that increase intracellular $[Na^+]$ have been reported to increase the size of the $[Ca^{2+}]_i$ transient (28) and the strength of contraction (29). In the four cells tested, voltage-clamp pulses of 50 ms duration from −70 to +10 mV delivered at 0.2 Hz led to an average Δf_{DCa} of 3.7 ± 0.4%, which corresponds to a peak $\Delta[Ca^{2+}]_i$ of 2.0 μM. This represents an increase of 30% over the average size of the $[Ca^{2+}]_i$ transients observed with pipette solutions containing 0 mM NaCl. In summary, during three separate experimental maneuvers, changes in the furaptra fluorescence transient were consistent with anticipated changes in the $[Ca^{2+}]_i$ transient. Thus, we conclude that the furaptra transient is a measure of the change in the size of the $[Ca^{2+}]_i$ transient.

Effect of intracellular $[Mg^{2+}]$ on the size of the furaptra fluorescence transient

Furaptra was originally designed as a Mg^{2+} indicator (12). Thus, a pertinent question is whether changes in $[Mg^{2+}]_i$ contribute to the furaptra fluorescence transient and, thereby, confound the calibration of fluorescence changes in terms of $[Ca^{2+}]_i$. The changes in $[Mg^{2+}]_i$ during $[Ca^{2+}]_i$ transients have not been directly examined in cardiac muscle. This is due largely to the fact that Mg^{2+} indicators, including furaptra, are also Ca^{2+}-sensitive, so that during rapid changes in $[Ca^{2+}]_i$, it is not possible to unequivocally determine $[Mg^{2+}]_i$. There is reason to believe, however, that $[Mg^{2+}]_i$ does change, at least somewhat, during the $[Ca^{2+}]_i$ transient because there are many buffer species in the cell where Ca^{2+} and Mg^{2+} can compete (see Table 1). These buffer species include the Ca^{2+}/Mg^{2+} sites on troponin and myosin as well as sites on ATP, phosphocreatine, and calmodulin. As shown in Table 1, the potential sites in the cell where Ca^{2+} can compete with Mg^{2+} are quite numerous.

Our inability to experimentally examine $[Mg^{2+}]_i$ led us to develop a computer model to estimate what changes in $[Mg^{2+}]_i$ accompany changes in $[Ca^{2+}]_i$. The goal of these simulations was to estimate the extent to which changes in $[Mg^{2+}]_i$ contribute to the amplitude of the furaptra fluorescence transient so that any error in the calculation of change in $[Ca^{2+}]_i$ might be assessed. The model assumed the cytosolic space accessible to furaptra is represented by a single compartment containing furaptra and buffer species (Fig. 5). Ca^{2+} and Mg^{2+} binding to the buffer species (B) and furaptra (D) were calculated by simultaneously solving the following equations for each buffer using an Euler's numerical integration routine (30):

$$\frac{dBCa(t)}{dt} = B(t)\cdot Ca(t)\cdot k_{f,Ca} - BCa(t)\cdot k_{r,Ca} \qquad (5)$$

$$\frac{dBMg(t)}{dt} = B(t)\cdot Mg(t)\cdot k_{f,Mg} - BMg(t)\cdot k_{r,Mg}. \qquad (6)$$

Forward rate constants for Ca^{2+} ($k_{f,Ca}$) and Mg^{2+} ($k_{f,Mg}$) were assumed to be 1.25 e + 08 M^{-1} s^{-1} and 3.33 e + 04

TABLE 1 Ca^{2+}/Mg^{2+} Buffers

Species	Concentration	K_D	k_f	k_r
	μmol/liter	*M*	$M^{-1}\ s^{-1}$	s^{-1}
Furaptra				
Ca	300	4.7e-05	1.25e08	5,875
Mg		3.6e-03	3.33e04	120
Troponin				
Ca	2 × 70	3.3e-09	1.0e08	0.33
Mg		3.3e-05	3.33e04	1.11
Myosin				
Ca	2 × 70	3.33e-08	1.37e07	0.46
Mg		3.64e-04	1.57e04	0.057
CaMod 1				
Ca	6	1.88e-06	1.25e08	235
Mg		1.96e-03	3.33e04	64.7
CaMod 2				
Ca	6	1.84e-06	1.25e08	230
Mg		2.92e-03	3.33e04	96.4
CaMod 3				
Ca	6	7.49e-06	1.25e08	938
Mg		1.25e-03	3.33e04	51.3
CaMod 4				
Ca	6	6.14e-05	1.25e08	7,675
Mg		6.14e-03	3.33e04	203
ATP				
Ca	3,000	2.0e-04	1.25e08	2.5e04
Mg		9.0e-05	3.33e04	3.0
P-Creatine				
Ca	12,000	7.1e-02	1.25e08	8.9e06
Mg		5.0e-02	3.33e04	1,670

The values for intrinsic buffer concentrations are expressed as micromole per liter accessible cell water and equilibrium dissociation constants (K_D) are taken from Fabiato (33). Diffusion-limited on-rate constants (k_f) are taken from Robertson et al. (32) to calculate off-rate constants (k_r). The concentration of furaptra is assumed to be equal to the electrode concentration and off-rate constants are calculated assuming diffusion-limited on-rate constants. The two sites on myosin and troponin C are assumed to behave identically and the four sites on calmodulin (CaMod1-4) are assumed to behave independently. ATP and phosphocreatine (P-Creatine) are included without accounting for the low cellular concentrations of dephosphorylated metabolites that are present in the normal intracellular environment.

$M^{-1}\ s^{-1}$, respectively. Reverse rate constants ($k_{r,Ca}$, $k_{r,Mg}$) were taken from Holroyde et al. (31) and Robertson et al. (32) or calculated from equilibrium binding constants (33). The concentration of the buffer species, taken from Fabiato (33), equaled the sum of the Ca^{2+}-bound (BCa), Mg^{2+}-bound (BMg), and unbound forms (B) of the buffer, and the concentration of furaptra was assumed to equal the pipette concentration. The step size (Δt) was reduced until no change in the numerical solution was observed. When necessary $Ca(t + \Delta t)$ was determined by linearly interpolating between consecutive data points.

A sample $[Ca^{2+}]$ transient used as the driving function in these calculations is shown in Fig. 6 *A*. The $[Ca^{2+}]$ transient was measured in a myocyte loaded with fura-2 because this indicator has a very low affinity for Mg^{2+} (2), so that the timecourse of the transient reflects only changes in $[Ca^{2+}]$. However, the experimental conditions and the voltage clamp protocol were the same as those used in Fig. 3. The $[Ca^{2+}]$ transient was obtained from the fura-2 fluorescence signal as described previously (23) except for a scaling factor that left resting $[Ca^{2+}]$ unchanged at 35 nM but increased peak $[Ca^{2+}]$ to 2.0 μM, similar to the size of the $[Ca^{2+}]_i$ transients determined with furaptra.

Simulations were run at two initial $[Mg^{2+}]$, 0.5 mM (Fig. 6, *left panels*) and 2.0 mM (*right panels*). Total intracellular Mg^{2+} was the sum of Mg^{2+} bound to the intracellular buffers and $[Mg^{2+}]$. The value of total Mg^{2+}, calculated at $t = 0$ by assuming $[Mg^{2+}]$ and $[Ca^{2+}]$ were in equilibrium with all buffers, was held constant throughout the calculation, i.e., there is no net entry or efflux of Mg^{2+} from the cytosol (see Discussion). Buffers with slow binding rate constants, such as myosin and troponin (see Table 1), necessitated that the simulation be run several times before consecutive $[Ca^{2+}]$ transients produced repeatable changes in Ca^{2+} and Mg^{2+} binding. Fig. 6, *B–F*, therefore, show the time course of binding only during the last $[Ca^{2+}]$ transient of the entire simulation.

Fig. 6, *B* and *C*, shows the calculated changes in Mg^{2+} binding to calmodulin and Ca^{2+}/Mg^{2+} sites of troponin, respectively. Calmodulin is shown as an example of a fast buffer, in rapid equilibrium throughout most of the $[Ca^{2+}]_i$ transient, so that the time course of changes in Mg^{2+} binding closely approximate changes in $[Ca^{2+}]$. The fast buffers also include ATP, phosphocreatine, and furaptra. At the peak of the $[Ca^{2+}]$ transient only a very small amount of Mg^{2+} is displaced from calmodulin (a total of 1.2 μM with 0.5 mM $[Mg^{2+}]$ and 2.3 μM with 2.0 mM $[Mg^{2+}]$) because calmodulin is predominantly in the metal-free state at resting $[Ca^{2+}]_i$. Thus, the rapid increase in $[Ca^{2+}]$ results in Ca^{2+} binding largely to the

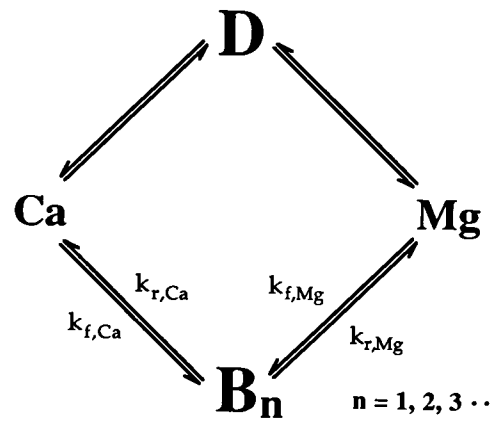

FIGURE 5 Model for Ca^{2+} and Mg^{2+} competition within a myocyte. Furaptra, *D*, and cellular buffers, *B* (see Table 1), can bind either Ca^{2+} or Mg^{2+}, assuming 1-to-1 binding stoichiometry. Buffer species with multiple binding sites are assumed to show independence between sites. The myoplasmic space accessible to Mg^{2+} and Ca^{2+} is assumed to consist of a single, identical compartment with instantaneous mixing.

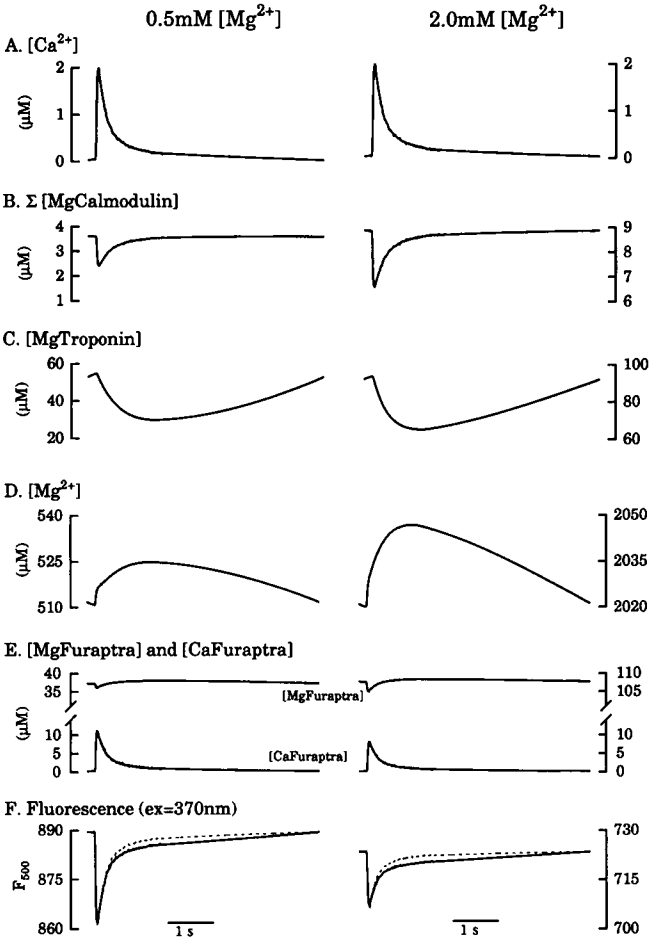

FIGURE 6 Results of simulations examining how Ca^{2+} and Mg^{2+} competition affects furaptra fluorescence. *The lefthand panels* are from a simulation performed with an initial $[Mg^{2+}]$ of 0.5 mM and *the righthand panels* are from an identical simulation run with 2.0 mM $[Mg^{2+}]$. For some panels, the values on the vertical axis of the *left-* and *righthand panels* are different, but the increment along the axis is the same. All records displayed are from the last of the three repeats of the simulation calculations needed to achieve steady-state conditions in the model. (*A*) The $[Ca^{2+}]$ transient used as a driving function for the simulation. The $[Ca^{2+}]$ transient is scaled so that peak $[Ca^{2+}]$ is 2.0 μM and resting $[Ca^{2+}]$ is 35 nM. The transient was recorded from a cell voltage clamped with the electrode solution (see Methods) containing 50 μM fura-2 (K^+-salt) and depolarized from −70 to +10 mV for 50 ms at 0.2 Hz. (*B*) Mg^{2+} binding to calmodulin. The sum of Mg^{2+} binding to all four sites of calmodulin is displayed. Total binding site concentration is 24 μM/liter cell myoplasm. (*C*) Mg^{2+} binding to troponin. The sum of Mg^{2+} binding to the 2 Ca^{2+}/Mg^{2+} binding sites of troponin is displayed. The total number of binding sites is 140 μM/liter cell myoplasm. (*D*) $[Mg^{2+}]$ transient. (*E*) Ca^{2+} binding and Mg^{2+} binding to furaptra. (*F*) Predicted furaptra fluorescence. The solid lines show the change in furaptra fluorescence predicted from the changes in [MgFuraptra] and [CaFuraptra] in *E*, assuming total furaptra is 300 μM. Fluorescence was calculated using Eq. 7 and the molar fluorescence coefficients from Fig. 1 (see text). The dashed lines were calculated after repeating the simulations except that $[Mg^{2+}]$ was held constant at 0.51 (*left*) and 2.02 mM (*right*).

unbound calmodulin. In general, increasing the concentration of fast Mg^{2+} binding sites improved the buffering of free Mg^{2+} and decreased the amplitude of the $[Mg^{2+}]$ transient without significantly altering its time course. Fast Mg^{2+} buffers do not appear to be major sites for competition between Mg^{2+} and Ca^{2+}. Fig. 6 *C* shows the time course of changes in Mg^{2+} binding to the two Mg^{2+}/Ca^{2+} sites of troponin (both sites are assumed to have identical rate constants). Because of the slow Mg^{2+} off-rates, these sites respond slowly to changes in $[Ca^{2+}]$, i.e., changes in Mg^{2+} binding lag far behind the $[Ca^{2+}]$ transient. The large amount of Mg^{2+} displaced from troponin (26 μM with 0.5 mM $[Mg^{2+}]$ and 29 μM with 2.0 mM $[Mg^{2+}]$) occurs because this buffer is almost completely bound with either Ca^{2+} or Mg^{2+}. Additional Ca^{2+} binding, therefore, occurs only after displacement of bound Mg^{2+}. Thus, most competition between Mg^{2+} and Ca^{2+} occurs at sites on slow buffers such as troponin and myosin.

The domination of competition between Mg^{2+} and Ca^{2+} by slow buffers suggests that displacement of bound Mg^{2+} from these buffers will dominate the change in $[Mg^{2+}]$ during the $[Ca^{2+}]$ transient. In fact, our calculations predict that the peak change in $[Mg^{2+}]$ occurs >1 s after the beginning of the $[Ca^{2+}]$ transient (Fig. 6 *D*). The size of the change in $[Mg^{2+}]$ is small (14 μM with 0.5 mM $[Mg^{2+}]$ and 29 μM with 2.0 mM $[Mg^{2+}]$), principally because ATP binds with a significant fraction of the displaced Mg^{2+}. At the time of the peak change in $[Ca^{2+}]$, $[Mg^{2+}]$ has increased only slightly. Thus, changes in $[Mg^{2+}]_i$ are predicted to be small, even in response to a large $[Ca^{2+}]_i$ transient.

Fig. 6 *E* shows the changes in Ca^{2+} and Mg^{2+} binding to furaptra. Because furaptra is a fast buffer for Ca^{2+}, and likely a fast buffer of Mg^{2+}, it is not surprising that the simulation predicts that divalent cation binding to the indicator closely follows the time course of the $[Ca^{2+}]$ transient and the slow changes in $[Mg^{2+}]$. At the time of the peak of the $[Ca^{2+}]$ transient, Mg^{2+} binding to furaptra decreases rather than following the initial rise in $[Mg^{2+}]$, because the competition between Ca^{2+} and Mg^{2+} more than offsets the increase in Mg^{2+} binding that would be expected from the slight rise in $[Mg^{2+}]$. The amount of Ca^{2+} binding to furaptra decreases with 2.0 mM $[Mg^{2+}]$, consistent with an increase in the apparent K_D for Ca^{2+} at higher Mg^{2+} concentrations.

The amount of Ca^{2+} and Mg^{2+} binding to the indicator was used to calculate predicted furaptra fluorescence transients during 370 nm illumination with the following equation:

$$Fl_{370}(t) = \epsilon_{b,Ca} \cdot DCa(t) + \epsilon_{b,Mg} \cdot DMg(t) + \epsilon_f \cdot D(t), \quad (7)$$

where $\epsilon_{b,Ca}$ and $\epsilon_{b,Mg}$ are the fluorescence coefficients for the Ca^{2+}- and Mg^{2+}-bound forms of furaptra during illumination with 370 nm light, respectively (see Fig. 1). The predicted fluorescence transients calculated in this

manner are shown in Fig. 6 *F* (*solid lines*). As expected from Fig. 6 *E*, the magnitude of the transient is decreased with higher basal $[Mg^{2+}]$. Expressed as Δf_{DCa} (not shown), the magnitude of the predicted fluorescence transients is 3.60% with 0.5 mM $[Mg^{2+}]$ and 2.63% with 2.0 mM $[Mg^{2+}]$. To examine whether changes in $[Mg^{2+}]$ have a significant effect on the fluorescence transient, we repeated simulations in which $[Mg^{2+}]$ was held constant (*dashed lines* in Fig. 6 *F*). The peak change in fluorescence predicted when $[Mg^{2+}]$ was held constant is very similar to that predicted when $[Mg^{2+}]$ was allowed to vary, as in Fig. 6 *D*. These simulations point out that *a*) only after $[Ca^{2+}]$ has returned near basal levels would the $[Mg^{2+}]$ transient have a significant effect on the fluorescence transient, and *b*) changes in furaptra fluorescence at the peak of the transient appear to be due overwhelmingly to changes in $[Ca^{2+}]$ with little interference from the $[Mg^{2+}]$ transient.

DISCUSSION

Use of furaptra as a Mg^{2+} indicator

Furaptra was originally synthesized for use as an indicator of $[Mg^{2+}]_i$ (12). Clearly, the results of Konishi et al. (11) and those of the present paper demonstrate that furaptra is also a useful indicator for monitoring changes in $[Ca^{2+}]_i$ in skeletal and cardiac muscle. This raises the general issue of how to interpret changes in furaptra fluorescence. The selectivity of furaptra for Ca^{2+} over Mg^{2+} appears to be temperature dependent (27-fold at 37°C, Raju et al. (12); 75-fold at room temperature, present report; 120-fold at 16°C, Konishi et al. (11)) due to an inverse relation between temperature and the affinity for Mg^{2+}. Thus, at lower temperatures, furaptra becomes a progressively better Ca^{2+} indicator because changes in $[Mg^{2+}]_i$ produce a smaller change in fluorescence. In skeletal (34) and cardiac muscle, the kinetics and the waveform for changes in $[Ca^{2+}]_i$ and $[Mg^{2+}]_i$ during a stimulated $[Ca^{2+}]_i$ transient also appear to be different, so that changes in fluorescence arising from changes in $[Ca^{2+}]_i$ and $[Mg^{2+}]_i$ can be easily distinguished. In cells where $[Ca^{2+}]_i$ and $[Mg^{2+}]_i$ tend to change slowly, particularly at higher temperatures, it may become difficult to clearly identify changes in fluorescence with a change in concentration of either cation.

Use of furaptra as a Ca^{2+} indicator

To use furaptra as a Ca^{2+} indicator, it was necessary to establish that changes in $[Ca^{2+}]_i$ could be measured reliably without contamination by movement artifact and changes in $[Mg^{2+}]_i$. Cleeman and Morad (13) have presented preliminary data that furaptra could be used as a Ca^{2+} indicator in cardiac myocytes; however, $[Ca^{2+}]_i$-dependent changes in fluorescence could be identified in only 5 of 15 cells examined. Such a low success rate would call into question the reliability of measurements made with furaptra. In this study, we did not have similar problems, as 91% of the cells loaded with furaptra demonstrated $[Ca^{2+}]_i$-dependent fluorescence transients. The apparent improvement may reflect our attempt to maximize the signal-to-noise ratio of the fluorescent signals by signal averaging records and by recording fluorescence from the entire cell. In addition, we found that three experimental maneuvers (increased depolarization duration, increased pipette $[Na^+]$, and exposure to isoproterenol) all led to increases in the size of the fluorescence transient consistent with expected increases in the size of the $[Ca^{2+}]_i$ transient. Thus, our results show that furaptra can be a reliable indicator for stimulated $[Ca^{2+}]_i$ transients.

Movement artifacts were a problem in the data reported by Cleeman and Morad (13). In the present study, movement artifacts as large or larger than the cation-dependent changes in the raw fluorescence signal were removed or minimized by multiplying the raw fluorescence signal recorded during 370 nm illumination by the relative change in fluorescence recorded during 350 nm illumination, close to the isosbestic point. Nonetheless, even in the raw fluorescence signal, movement artifacts did not completely obscure the Ca^{2+}-dependent changes in fluorescence because the peak of the $[Ca^{2+}]_i$ transient was reached before cell movement became large. The other possible complication, that changes in $[Mg^{2+}]_i$ concentration would significantly change the amplitude of the furaptra fluorescence transient, also did not appear likely (see below). Thus, changes in $[Ca^{2+}]_i$ at the peak of the transient could be reliably measured and calibrated using furaptra as the Ca^{2+} indicator.

Only stimulated $[Ca^{2+}]_i$ transients were examined in the present study. Such transients tend to be stereotyped events (16) which are characterized by uniform increases in $[Ca^{2+}]_i$ throughout the cell (35). However, isolated rat myocytes are particularly prone to the appearance of spontaneous oscillations of cell length (36) and $[Ca^{2+}]_i$ (16). If such spontaneous oscillations were present, the myocytes were excluded from analysis because the stimulated $[Ca^{2+}]_i$ transients show marked beat-to-beat variability (16), which precludes meaningful signal averaging. We nonetheless attempted to calibrate the spontaneous oscillations in fluorescence that were observed under such conditions by the single wavelength calibration technique discussed in Berlin et al. (16); however, the low signal-to-noise ratio prevented any useful calibration. A disadvantage of furaptra, therefore, is that its utility is limited to measuring changes in $[Ca^{2+}]_i$ under steady-state conditions where the $[Ca^{2+}]_i$ transient remains a stereotyped event.

Changes in $[Mg^{2+}]_i$ during the $[Ca^{2+}]_i$ transient

Lacking a means to experimentally examine changes in $[Mg^{2+}]_i$ during the $[Ca^{2+}]_i$ transient, we developed a computer simulation to predict how changes in $[Mg^{2+}]_i$

could affect the fluorescence recorded with furaptra. The concentrations of Mg^{2+} and Ca^{2+} buffers were taken from literature values (33). These values seem reasonable in light of the report of Sipido and Wier (37), whose data suggested that the intrinsic Ca^{2+} buffering capacity of a cardiac myocyte is close to the value published in Fabiato (33). Thus, the concentrations of the buffers used in the present simulations for Ca^{2+}/Mg^{2+} competition, particularly calmodulin and troponin, may not be greatly different from the cellular concentration.

The concentration of furaptra was assumed to be equal to the electrode concentration. This value may actually be a lower-end estimate, inasmuch as fluorescence measurements were taken when dye loading was near equilibrium. Approximately 50% of cellular furaptra appears to be bound to intracellular macromolecules in skeletal muscle fibers (3). Cellular binding has a relative concentrating effect on fura-2 (14) and indo-1 in myocytes (5). Thus, at equilibrium, cellular furaptra concentration may exceed the electrode concentration.

An important assumption of the model is that total myoplasmic Mg^{2+} remains constant throughout the $[Ca^{2+}]_i$ transient. This assumption could be invalid if large amounts of Mg^{2+} move into and out of the sarcoplasmic reticulum and the mitochondria or across the sarcolemma. Hogue and Hansford (38) showed that millimolar changes in extramitochondrial $[Mg^{2+}]$ did not significantly alter matrix $[Mg^{2+}]$ in mitochondria isolated from rat heart. Thus, Mg^{2+} flux across the mitochondrial membrane is probably not an important consideration in the model calculations. The ability of Mg^{2+} to move across the sarcoplasmic reticulum membrane was examined by Somlyo et al. (39). These authors demonstrated that sarcoplasmic reticulum Mg^{2+} content increased with prolonged tetanic stimuli in skeletal muscle. The amount of Mg^{2+} that would move across the reticular membrane in response to a single stimulation is probably much smaller. Even so, in terms of the model, any Mg^{2+} movement into the sarcoplasmic reticulum would decrease the total myoplasmic Mg^{2+} and, therefore, decrease the free Mg^{2+} transient. Finally, there are Mg^{2+} transport mechanisms in the cardiac sarcolemma that appear to change $[Mg^{2+}]_i$ only very slowly (reviewed by Murphy [40]). These considerations lead us to conclude that, over the time course of our simulations, the assumption of constant total myoplasmic Mg^{2+} would not lead to an underestimate of changes in $[Mg^{2+}]_i$.

The simulations predict that the $[Mg^{2+}]_i$ transient following a 2.0 μM $[Ca^{2+}]_i$ transient will be 14–26 μM (basal $[Mg^{2+}]_i$ 0.5–2.0 mM) and reach peak amplitude $\sim$1 s after the beginning of the $[Ca^{2+}]_i$ transient. Kirschenlohr et al. (41) have attempted to measure changes in $[Mg^{2+}]_i$ during the cardiac cycle with gated ^{19}F-NMR to examine Mg^{2+} binding to (+)-fluorocitrate. These authors could find no significant change in $[Mg^{2+}]_i$ with ferret hearts paced at 1.25 Hz. The lack of any change in $[Mg^{2+}]_i$ could reflect the short cycle length for pacing; however, it could also represent a methodological problem. The probe was loaded as the acetoxy methyl ester, and this method of loading often results in a sizable fraction of the probe residing in the mitochondria which, as discussed above, is not likely to have a $[Mg^{2+}]_i$ transient. Thus, the results of Kirschenlohr et al. (41) should be interpreted as ruling out very large changes in $[Mg^{2+}]_i$ during the transient. Our model calculations also suggest that large changes in $[Mg^{2+}]_i$ are unlikely.

Changes in $[Mg^{2+}]_i$ following $[Ca^{2+}]_i$ transients in skeletal muscle have been examined by determining non-Ca^{2+}-dependent changes in antipyrylazo III absorbance (34, 42). These authors report that $[Mg^{2+}]_i$ increases $\sim$60 μM in response to a single stimulus. A comparison with cardiac muscle is difficult because the increase in $[Mg^{2+}]_i$ in skeletal muscle appears to occur largely because Ca^{2+} displaces Mg^{2+} from parvalbumin (34), a protein that appears to be almost absent in rat cardiac cells (43). Nonetheless, the amount of Ca^{2+} involved in a skeletal muscle $[Ca^{2+}]_i$ transient (44) is several times that in a cardiac muscle $[Ca^{2+}]_i$ transient (9, 45), so that the $[Mg^{2+}]_i$ transient in skeletal muscle probably represents an upper-end estimate for that in cardiac muscle.

The present model for $[Mg^{2+}]_i$ in cardiac cells does demonstrate that slow buffer species, particularly troponin, dominate the change in $[Mg^{2+}]_i$ in response to a $[Ca^{2+}]_i$ transient. This occurs because a significant fraction of fast, low-affinity buffer species exist in metal-free form, whereas the high-affinity, slow buffers are almost completely Mg^{2+} or Ca^{2+} bound. An increase in $[Ca^{2+}]_i$, therefore, leads to displacement of Mg^{2+} from the slow buffers with consequent Mg^{2+} binding to fast buffer species, quite similar to the case in skeletal muscle. In terms of affecting the furaptra fluorescence transient, the slow changes in $[Mg^{2+}]_i$ mean that the peak of the fluorescence transient will not be significantly altered by changes in $[Mg^{2+}]_i$. Fig. 6 *F* also predicts, however, that changes in $[Mg^{2+}]_i$ could affect the later phases of the transient when $[Ca^{2+}]_i$ has returned to near basal levels.

Comparison of $[Ca^{2+}]_i$ transients determined with furaptra and other indicators

Several indicators are now available to measure the $[Ca^{2+}]_i$ in the heart, including aequorin, the ratiometric fluorescent indicators such as fura-2 and indo-1, ^{19}F-BAPTA for gated nuclear magnetic resonance (NMR), and nonratiometric indicators such as fluo-3 and calcium-X (Crimson, Green, et cetera). Despite the fact that the experimental conditions under which these different indicators have been used are quite varied and that the assumptions involved in calibration are different, it is interesting to compare the $[Ca^{2+}]_i$ transients reported by some of the more commonly used indicators with those reported by furaptra.

As shown in Figs. 2 and 3, one advantage of furaptra is that calibration in terms of $[Ca^{2+}]_i$ is relatively straightforward. The binding stoichiometry is 1:1 and, in the range of $[Ca^{2+}]_i$ encountered in the present study, only a small fraction of the total indicator binds with Ca^{2+}. Thus, changes in fluorescence during 370 nm illumination are linear with spatial mean $[Ca^{2+}]_i$ (Fig. 3). In the presence of rapid changes of $[Ca^{2+}]_i$ during the transient, furaptra will also accurately report $[Ca^{2+}]_i$ because of the indicator's low Ca^{2+} affinity. In regards to this point, experiments in skeletal muscle fibers have shown that the time course of the furaptra fluorescence transient is much faster than that for high-affinity indicators such as fura-2 (11). These advantages of furaptra, however, must be weighed against the disadvantage of the low signal-to-noise ratio and the Mg^{2+} sensitivity of this indicator.

Eq. 4 also shows that a source of error in the calibration procedure is the determination of K_D. For the present experiments, K_D was determined *in vitro* and then corrected for Mg^{2+} competition. It is unlikely, however, that this accurately reflects the affinity of furaptra for Ca^{2+} in the cell. Furaptra is reported to be 50% bound in skeletal muscle (11), and binding to proteins appears to decrease the Ca^{2+} affinity of furaptra severalfold (Mapp, A. K., and J. R. Berlin, unpublished observations), similar to the effect of protein binding on fura-2 (3) and indo-1 (5). Thus, assuming furaptra also binds to intracellular constituents in cardiac myocytes, the reported changes in $[Ca^{2+}]_i$ should be considered lower-end estimates of the true change in $[Ca^{2+}]_i$.

$[Ca^{2+}]_i$ transients in electrically stimulated ventricular muscle preparations measured with aequorin have generally been reported to be 1–2 μM in amplitude under a wide variety of experimental conditions (1, 9), similar to the size of the transient reported with furaptra. Generally, two problems are recognized with aequorin estimates of $[Ca^{2+}]_i$. First, like furaptra, Mg^{2+} has important effects on Ca^{2+}-dependent luminescence. Many previous calibrations of aequorin luminescence assumed $[Mg^{2+}]_i$ to be 2–3 mM, whereas recent estimates suggest that the value is closer to 0.5–1.0 mM (40). Mg^{2+} inhibits the Ca^{2+} reaction with aequorin (46) in such a way that, with $[Ca^{2+}]$ below 3 μM, decreased estimates of $[Mg^{2+}]_i$ would simply scale down the size of the transient. The magnitude of the resulting overestimation of $[Ca^{2+}]_i$, however, could be as large as 50–75% (47). The more widely appreciated problem with aequorin is due to the steep dependence of luminescence on $[Ca^{2+}]$ (46). In the presence of spatial gradients of $[Ca^{2+}]_i$, which are likely to be present during rapid release of Ca^{2+} from the sarcoplasmic reticulum (8, 9), aequorin will overestimate $[Ca^{2+}]_i$. Wier and Yue (9) carried out simulations using a 1-μM $[Ca^{2+}]$ transient and found that the magnitude of this overestimation to be 7%. However, with transients as large as those reported by furaptra, more pronounced spatial gradients of $[Ca^{2+}]_i$ may exist so that the true overestimation of $[Ca^{2+}]_i$ may be much greater. Consideration of inaccurate estimates of $[Mg^{2+}]_i$ and the steep $[Ca^{2+}]_i$ dependence of luminescence suggest that many previous estimates of $[Ca^{2+}]_i$ with aequorin could produce an overestimate of size of the $[Ca^{2+}]_i$ transient. Thus, the $[Ca^{2+}]_i$ transient reported by furaptra represents a change in $[Ca^{2+}]_i$ that is as large or larger than that reported by aequorin.

In contrast with aequorin, Ca^{2+} indicators such as indo-1, fura-2, and ^{19}F-BAPTA tend to underestimate the true size of the $[Ca^{2+}]_i$ transient. These indicators bind Ca^{2+} with 1:1 stoichiometry and have *in vitro* dissociation constants of 100–300 nM (2). Thus, one disadvantage of these indicators is that, during rapid release of sarcoplasmic reticulum Ca^{2+}, spatial gradients of $[Ca^{2+}]_i$ are likely to exist (8, 9), which could lead to significant saturation of the indicator and underestimation of spatial mean $[Ca^{2+}]$ (10). If the affinity of these indicators for Ca^{2+} in the cell is decreased (3, 5), dye saturation may be less severe than anticipated. Nonetheless, calibrations that use the K_D determined *in vitro* are still likely to underestimate $[Ca^{2+}]_i$.

Given the above reservations, we can compare the size of $[Ca^{2+}]_i$ transients reported with furaptra and ^{19}F-BAPTA or fura-2. Kusuoka et al. (48) used gated NMR with ^{19}F-BAPTA-loaded ferret hearts stimulated at 0.8–1.4 Hz to determine that the average change in $[Ca^{2+}]_i$ near the peak of the transient was 430 and 780 nM (control and postischemia, respectively). The advantage of this technique is that the relative amount of bound and free ^{19}F-BAPTA can be determined directly from the area under the peaks of the NMR spectra. By comparison, calibration of fura-2 and indo-1 also requires the determination of the fluorescence ratios in Ca^{2+}-free (R_{min}) and saturating Ca^{2+} conditions (R_{max}). The work of Li et al. (49) suggests that R_{min} and R_{max} in myocytes may be different than under *in vitro* conditions. Nonetheless, using *in vitro* calibration techniques, the amplitude of the $[Ca^{2+}]_i$ transient determined with fura-2 is only one fourth as large as the transient determined with furaptra under the same conditions (14). The reasons for this apparent discrepancy need to be examined more thoroughly before it is possible to conclude that fura-2 and furaptra report different $[Ca^{2+}]_i$.

Several nonratiometric fluorescent Ca^{2+} indicators such as fluo-3 and the calcium-X analogues have also been introduced. Some of these indicators have the advantage of Ca^{2+} affinities intermediate to those of fura-2 and furaptra but with extremely low affinities for Mg^{2+}. The inability to correct for movement artifacts, however, will limit the utility of these indicators and may explain why they have not been used extensively to quantitate changes in $[Ca^{2+}]_i$ during cell contraction.

In summary, several Ca^{2+} indicators are available to measure $[Ca^{2+}]_i$ in cardiac myocytes, each with its own advantages and disadvantages. Furaptra, with the lowest Ca^{2+} affinity, is useful for large and rapid $[Ca^{2+}]_i$ tran-

sients that are stereotyped events. Fura-2 and indo-1 are particularly useful for smaller changes in $[Ca^{2+}]_i$ that may not be reproducible. Uncertainties remain in the calibration procedures for these indicators. However, given the relative simplicity of the calibration procedure used for furaptra, the size of the $[Ca^{2+}]_i$ transient reported in the present study should be considered at least as accurate as other methods. Thus, the size of the $[Ca^{2+}]_i$ transient determined with furaptra is as large or larger than that determined with other Ca^{2+} indicators. Furthermore, measurements of peak changes in $[Ca^{2+}]_i$ with furaptra appear to be reliable and without significant interference from Mg^{2+}.

We acknowledge the excellent technical assistance of Anna K. Mapp and Alexander J. Fielding. We thank Stephen M. Baylor for helpful discussions and comments on an earlier version of the manuscript and Satoshi Kurihara for reviewing the final manuscript.

This work was supported by grants from the National Institutes of Health (HL-43712) and the Southeastern Pennsylvania affiliate of the American Heart Association to J. R. Berlin.

Received for publication 29 April 1992 and in final form 19 October 1992.

REFERENCES

1. Allen, D. G., and J. R. Blinks. 1978. Calcium transients in aequorin-injected frog cardiac muscle. *Nature (Lond.)*. 273:509–513.
2. Grynkiewicz, G., M. Poenie, and R. Y. Tsien. 1985. A new generation of Ca^{2+} indicators with greatly improved fluorescence properties. *J. Biol. Chem.* 260:3440–3450.
3. Konishi, M., A. Olson, S. Hollingworth, and S. M. Baylor. 1988. Myoplasmic binding of fura-2 investigated by steady-state fluorescence and absorbance measurements. *Biophys. J.* 54:1089–1104.
4. Blatter, L. A., and W. G. Wier. 1990. Intracellular diffusion, binding and compartmentalization of the fluorescent calcium indicators indo-1 and fura-2. *Biophys. J.* 58:1491–1499.
5. Hove-Madsen, L., and D. M. Bers. 1992. Indo-1 binding to protein in permeabilized ventricular myocytes alters its spectral and Ca binding properties. *Biophys. J.* 63:89–97.
6. Klein, M. G., B. J. Simon, G. Szucs, and M. F. Schneider. 1988. Simultaneous recording of calcium transients in skeletal muscle using high and low affinity calcium indicators. *Biophys. J.* 53:971–988.
7. Baylor, S. M., and S. Hollingworth. 1988. Fura-2 calcium transients in frog skeletal muscle fibres. *J. Physiol. (Lond.)*. 403:151–192.
8. Cannell, M. B., and D. G. Allen. 1984. Model of calcium movements during activation in the sarcomere of frog skeletal muscle. *Biophys. J.* 45:913–925.
9. Wier, W. G., and D. T. Yue. 1986. Intracellular calcium transients underlying the short-term force-interval relationship in ferret ventricular myocardium. *J. Physiol. (Lond.)*. 376:507–530.
10. Marban, E., M. Kitakaze, Y. Koretsune, D. T. Yue, V. P. Chacko, and M. M. Pike. 1990. Quantification of $[Ca^{2+}]_i$ in perfused hearts. *Circ. Res.* 66:1255–1267.
11. Konishi, M., S. Hollingworth, A. B. Harkins, and S. M. Baylor. 1991. Myoplasmic calcium transients in intact frog skeletal muscle fibers monitored with the fluorescent indicator furaptra. *J. Gen. Physiol.* 97:271–301.
12. Raju, B., E. Murphy, L. A. Levy, R. D. Hall, and R. E. London. 1989. A fluorescent indicator for measuring cytosolic free magnesium. *Am. J. Physiol.* 256:C540–C548.
13. Cleeman, L., and M. Morad. 1991. Role of Ca^{2+} channel in cardiac excitation-contraction coupling in the rat: evidence from Ca^{2+} transients and contraction. *J. Physiol. (Lond.)*. 432:283–312.
14. Konishi, M., and J. R. Berlin. 1991. $[Ca^{2+}]_i$ transients in cardiac myocytes measured with high and low affinity calcium fluorescent indicators. *Biophys. J.* 59:542*a* (Abstr.).
15. Berlin, J. R., and M. Konishi. 1992. Effect of buffering and binding kinetics for fura-2 measurement of transient changes of Ca in cardiac myocytes. *Biophys. J.* 61:159*a* (Abstr.).
16. Berlin, J. R., M. B. Cannell, and W. J. Lederer. 1989. Cellular origins of the transient inward current in cardiac myocytes. *Circ. Res.* 65:115–126.
17. Mitra, R., and M. Morad. 1985. A uniform enzymatic method for dissociation of myocytes from hearts and stomachs of vertebrates. *Am. J. Physiol.* 249:H1056–H1060.
18. Cannell, M. B., and W. J. Lederer. 1986. A novel experimental chamber for single-cell voltage-clamp and patch-clamp applications with low electrical noise and excellent temperature and flow control. *Pfluegers Arch. Eur. J. Physiol.* 406:536–539.
19. Hamill, O. P., A. Marty, E. Neher, B. Sakmann, and F. J. Sigworth. 1981. Improved patch-clamp techniques for high-resolution recording from cells and cell-free membrane patches. *Pfluegers Arch. Eur. J. Physiol.* 391:85–100.
20. Fabiato, A., and F. Fabiato. 1979. Calculator programs for computing the composition of the solutions containing multiple metals and ligands used for experiments in skinned muscle cells. *J. Physiol. (Paris)*. 75:463–505.
21. Harrison, S. M., and D. M. Bers. 1987. The effect of temperature and ionic strength on the apparent Ca-affinity of EGTA and the analogous Ca-chelators BAPTA and dibromo BAPTA. *Biochim. Biophys. Acta.* 925:133–143.
22. Martell, A. E., and R. M. Smith. 1974. Critical Stability Constants. *In* Amino Acids. Vol. 1. Plenum Publishing Corp., New York. 199–269.
23. Cannell, M. B., J. R. Berlin, and W. J. Lederer. 1987. Effect of membrane potential changes on the calcium transient in single rat cardiac muscle cells. *Science (Wash. DC)*. 238:1419–1423.
24. Murphy, E., C. Steenbergen, L. A. Levy, B. Raju, and R. E. London. 1989. Cytosolic free magnesium levels in ischemic rat heart. *J. Biol. Chem.* 264:5622–5627.
25. Blatter, L. A., and J. A. McGuigan. 1988. Estimation of the upper limit of the free magnesium concentration measured with Mg-sensitive microelectrodes in ferret ventricular muscle. *Magnesium.* 7:154–165.
26. Berlin, J. R., M. B. Cannell, and W. J. Lederer. 1987. The dependence of the calcium transient on depolarization duration in voltage-clamped single heart cells. *Biophys. J.* 51:197*a* (Abstr.)
27. duBell, W. H., and S. R. Houser. 1989. Voltage and beat dependence of Ca^{2+} transient in feline ventricular myocytes. *Am. J. Physiol.* 257:H746–H759.
28. Hess, P., and W. G. Wier. 1984. Excitation-contraction coupling in cardiac Purkinje fibers. Effects of caffeine on the intracellular $[Ca^{2+}]$ transient, membrane currents, and contraction. *J. Gen. Physiol.* 83:417–433.
29. Eisner, D. A., W. J. Lederer, and R. D. Vaughan-Jones. 1984. The quantitative relationship between twitch tension and intracellular sodium activity in sheep cardiac Purkinje fibres. *J. Physiol. (Lond.)*. 355:251–266.

30. Simon, W. 1972. Mathematical Techniques for Physiology and Medicine. Academic Press, New York. 267 pp.

31. Holroyde, M. J., S. P. Robertson, J. D. Johnson, R. J. Solaro, and J. D. Potter. 1981. The calcium and magnesium binding sites of cardiac troponin and their role in the regulation of myofibrillar adenosine triphosphatase. *J. Biol. Chem.* 255:11688–11693.

32. Robertson, S. P., J. D. Johnson, and J. D. Potter. 1981. The time-course of Ca^{2+} exchange with calmodulin, troponin, parvalbumin, and myosin in response to transient increases in Ca^{2+}. *Biophys. J.* 34:559–569.

33. Fabiato, A. 1983. Calcium-induced release of calcium from the cardiac sarcoplasmic reticulum. *Am. J. Physiol.* 245:C1–C14.

34. Irving, M., J. Maylie, N. L. Sizto, and W. K. Chandler. 1989. Simultaneous monitoring in magnesium and calcium concentrations in frog cut twitch fibers containing Antipyrylazo III. *J. Gen. Physiol.* 93:585–608.

35. Cannell, M. B., J. R. Berlin, and W. J. Lederer. 1987. Intracellular calcium in cardiac myocytes: calcium transients measured using fluorescence imaging. *Soc. Gen. Physiol. Symp.* 42:202–214.

36. Kort, A. A., and E. G. Lakatta. 1984. Calcium-dependent mechanical oscillations occur spontaneously in unstimulated mammalian cardiac tissues. *Circ. Res.* 54:396–404.

37. Sipido, K., and W. G. Wier. 1991. Flux of Ca^{2+} across the sarcoplasmic reticulum of guinea-pig cardiac cells during excitation-contraction coupling. *J. Physiol. (Lond.)*. 435:605–630.

38. Hogue, B. A., and R. G. Hansford. 1990. Measurement of free Mg^{2+} in isolated heart mitochondria. *Biophys. J.* 57:186*a* (Abstr.)

39. Somlyo, A. V., G. McClellan, H. Gonzalez-Serratos, and A. P. Somlyo. 1985. Electron-probe X-ray microanalysis of post-tetanic Ca^{2+} and Mg^{2+} movements across the sarcoplasmic reticulum *in situ*. *J. Biol. Chem.* 260:6801–6807.

40. Murphy, E. 1991. Cellular magnesium and Na/Mg exchange in heart cells. *Annu. Rev. Physiol.* 53:273–287.

41. Kirschenlohr, H. L., J. C. Metcalfe, P. G. Morris, G. C. Rodrigo, and G. A. Smith. 1988. Ca^{2+} transient, Mg^{2+}, and pH measurements in the cardiac cycle by ^{19}F NMR. *Proc. Natl. Acad. Sci. USA.* 85:9017–9021.

42. Baylor, S. M., W. K. Chandler, and M. W. Marshall. 1982. Optical measurement of intracellular pH and magnesium in frog skeletal muscle fibres. *J. Physiol. (Lond.)*. 331:105–137.

43. Inaguma, Y., N. Kurobe, H. Shinohara, and K. Kato. 1991. Sensitive immunoassay for rat parvalbumin: tissue distribution and developmental changes. *Biochim. Biophys. Acta.* 1075:68–74.

44. Baylor, S. M., W. K. Chandler, and M. W. Marshall. 1983. Sarcoplasmic reticulum calcium release in frog skeletal muscle fibres estimated from arsenazo III calcium transients. *J. Physiol. (Lond.)*. 344:625–666.

45. Bers, D. M., W. J. Lederer, and J. R. Berlin. 1990. Intracellular Ca transients in rat cardiac myocytes: role of Na-Ca exchange in excitation-contraction coupling. *Am. J. Physiol.* 258:C944–C954.

46. Blinks, J. R., W. G. Wier, P. Hess, and F. G. Prendergast. 1982. Measurement of Ca^{2+} concentrations in living cells. *Prog. Biophys. Mol. Biol.* 40:1–114.

47. Blinks, J. R. 1989. Use of calcium-regulated photoproteins as intracellular Ca^{2+} indicators. *Methods Enzymol.* 172:164–203.

48. Kusuoka, H., Y. Koretsune, V. P. Chacko, M. L. Weisfeldt, and E. Marban. 1990. Excitation-contraction coupling in postischemic myocardium: does failure of activator Ca^{2+} transients underlie stunning? *Circ. Res.* 66:1268–1276.

49. Li, Q., R. A. Altschuld, and B. T. Stokes. 1987. Quantitation of intracellular free calcium in single adult cardiomyocytes by fura-2 fluorescence microscopy: calibration of fura-2 ratios. *Biochem. Biophys. Res. Commun.* 147:120–126.